https://doi.org/10.1016/j.atmosres.2008.04.012

Wavelet Multiresolution Based Multifractal Analysis of Electric Fields by Lightning Return Strokes

Xueqiang Gou[1,2], Mingli Chen[2], Yijun Zhang[3], Wansheng Dong[3], Xiushu Qie[4]

1. College of Physics and Electronic Engineering, Northwest Normal University, Lanzhou, Gansu, 730070, China
2. Department of Building Services Engineering, The Hong Kong Polytechnic University, Hong Kong, China
3. Chinese Academy of Meteorological Sciences, Beijing 100081, China
4 Institute of Atmospheric Physics, Chinese Academy of Sciences, Beijing 100029, China

Abstract: Lightning can be seen as a large-scale cooperative phenomenon, which may evolve in self-similar cascaded way. Using the electric field waveforms recorded by the slow antenna system, the mono- and multifractal behaviors of 115 first return strokes in negative cloud-to-ground discharges have been investigated with wavelet multi-resolution based multifractal method. The results show that the return stroke process, in term of its electric field waveform, has apparent fractality and strong degree of multifractality. The multifractal spectrums obtained for the 115 cases are all well fitted to a modified version of the binomial cascade multifractal model. The width of the multifractal spectrums, which measure the strength of multifractality, is 1.6 in average. The fractal dimension of the electric field waveforms ranges from 1.2 to 1.5 with an average of 1.3, a similar value to the fractal dimension of the lightning channel obtained by others. This suggests that the lightning-produced electric fields may appear the same fractal dimension as its channel. The relationship between the peak current of a return stroke and the charge deposition in its channel was also discussed. The results suggest that the wavelet and scaling analysis may be a powerful tool in interpretation of the lightning-produced electric fields and therefore in understanding of the lightning.

1. INTRODUCTION

The fine structure of electric field changes produced by a lightning return stroke is intensively studied for lightning protection interest (Bazelyan and Raizer, 2000; Uman, 2001).

∗ Correspondence to: Xueqiang Gou, Email: gouxueqiang@nwnu.edu.cn

Various features, such as the initial magnitude, zero crossing time, slow font duration and fast transition, are introduced to characterize the details of waveform of the lightning-produced electric field changes (Weidman and Krider, 1978; Cooray and Lundquist, 1985; Uman, 2001). However, the high variability of lightning, which is characterized with strong nonlinearity and multiple scales, often makes the analysis difficult (Davis, et al., 1994). On the other side, recent studies on theories of fractal suggested that large natural catastrophe, like lightning, can be considered as an emergent and collective phenomenon，which is governed by the universal law, implying that the important aspect of their behavior has little to do with the exact microscopic details such as physical, chemical, physiological, of the dynamic systems. This may provide a new perspective for the understanding of lightning process.

It is largely believed that the catastrophe is a self-organized system characterized with the scale invariant spatial fractal and temporal fluctuations (avalanche event), which may be two sides of the same coin, manifesting the self-organized evolution (Bak, 1987; Turcotte, et al, 2002). The analog to a critical phenomenon at a second-order phase transition suggested that the scaling behavior may be corrected by log-periodic oscillation, which is associated with complex exponent scaling law and the discrete scale invariance. This implies further that the large-scale hazard is controlled by their cooperativity and scaling up (inverse cascade) of their interactions and may potentially offer the prediction of natural disasters ((Turcotte et al., 2002; Sornette, 2002, 2004).

It is well established that lightning discharges follow a tortuous and brunching path (Kawasaki and Matsuura, 2000; Tan, et al., 2006). The work on the electromagnetic field radiated from a fractal channel show that the lightning channel may be considered as a fractal antenna (Vecchi, et al., 1994; Valdivia et al., 1997; Lupò et al., 2000). The tortuosity and branching of the discharge channel introduce profound modifications in the intensity and structure of the radiated electromagnetic field pattern (LeVine and Meneghini, 1978; Le Vine and Willett, 1995), and the radiated field appears the same fractal dimension as the channel (Vecchi, et al., 1994). Though there is much a difficult problem, the fractal behavior of lightning processes is utterly interesting topic indeed, especially considering its association with the possible criticality of lightning and their evolution. In this paper, by applying the wavelet multiresolution based multifractal method (Manimaran, et al., 2005, 2006) to the slow electric field change data (as recorded by the slow antenna), the fractal and multifractal properties of the electrical field radiated by lightning return strokes have been investigated.

2. METHOD

The nonlinear and cascade processes are usually associated with multifractality. Reliable identification of long-range correlation and the multifractality in real data is a difficult task mainly due to non-stationary of the data. One of the most widely used method of quantifying multifractal properties of time series in several fields is the multifractal detrended fluctuation analysis (MF-DFA) (Kantelhardt, et al., 2002), which is a generalization of the conventional detrended fluctuation analysis (DFA) approach commonly used in the analyses of scaling properties of signals in identifying correlations presented in noisy non-stationary time series (Peng, et al., 1994). The basic idea in the approach is to isolate fluctuations in the data set through multiple local windows or varying sizes.

Wavelet transforms are mathematical microscope (Daubechies, 1992; Mallat, 1999). The heart behind the wavelet transforms is the multiresolution analysis (see Appendix for details). With the wavelet multiresolution analysis, a signal can be decomposed into a coarse approximation (smooth background) and a series of details. The successive approximations can be used as the trend over a window size corresponding to different levels of wavelet decomposition. Thus, fluctuations can be extracted at each level by subtracting the above trend series from the original data. The built-in ability of the wavelet multiresolution analysis for capturing the trends and identifying the fluctuations around trends in variable window sizes in a data set makes it a natural tool for scaling processes.

The new wavelet based approach for multifractal method, which is very similar to that in MF-DFA, can be described as follows.

Step 1: For a given time series $x(i)$, $i=1,\ldots N$, determine the "profile", which is cumulative sum of the series subtracting the series mean value $<x>$.

$$Y(k) = \sum_{i=1}^{k} (x(i) - < x >) \quad (k = 1, ..., N) \tag{1}$$

Step 2: Carry out wavelet transforms on the profile $Y(i)$ and separate the fluctuations from the trend by considering precise values of window size corresponding to different levels of wavelet decomposition; Divide the fluctuations into $M_s = int(N/s)$ non-overlapping segments of length s starting from both the beginning and the end of the fluctuations series (i.e., $2Ms$ such segments in total); For each segment v at scale s, calculate the root mean square fluctuation function $F(v,s)$.

Step 3: Calculate the *q-th* order fluctuation function.

$$F_q(s) = \left(\frac{1}{2M_s} \sum_{v=1}^{2M_s} | F(v,s) |^q\right)^{1/q} \tag{2}$$

Step 4: Determine the scaling behavior of the *q-th* order fluctuation function $F_q(s)$ versus the s.

$$F_q(s) \sim s^{h(q)} \tag{3}$$

The scaling exponent *h(q)* is called generalized Hurst exponent. For positive values of *q*, *h(q)* describes the scaling behavior of the segments with large fluctuations, while those of negative values of *q* describe the scaling behavior of the segments with small fluctuations. For monofractal time series, *h(q)* is independent of *q*, whereas for a multifractal time series *h(q)* varies with *q*. Specifically, $H_1=h(1)$ is related to the graph dimension of signal $D=2-H_1$, and $H_2=h(2)$ is assumed to be identical to the well-known Hurst exponent *H* which is related to the power spectral analysis by the relation $\beta=2H+1$.

In comparison with the standard partition function based multifractal method, it can be easily verified that the term $\sum_{\nu=1}^{2M_s} |F(\nu,s)|^q$ is identical to the partition *Z(q,s)*, which behaves as the scaling law

$$Z(q,s) = \sum_{\nu=1}^{2M_s} |F(\nu,s)|^q \sim s^{\tau(q)} \tag{4}$$

Where *τ(q)* is the Renyi exponent, which is directly related to *h(q)* as the follow

$$\tau(q) + 1 = qh(q) \tag{5}$$

The singularity spectrum *f(α)* is related to *τ(q)* by the following relations

$$\begin{cases} \alpha(q) = \dfrac{d\tau(q)}{dq} \\ f(\alpha) = q\alpha(q) - \tau(q) \end{cases} \tag{6}$$

Where the *α* is the Hölder exponent and the *f(α)* is the Hausdorff dimension of the fractal subset with the exponent *α*. The strength of multifractality is measured with the width of exponents $\Delta\alpha = \alpha_{max} - \alpha_{min}$, which is the same as the width of the singular spectrum *f(α)* at *f=0*, the wider singularity spectrum, the stronger multifractality.

3. DATA AND RESULTS

3.1 **Data Acquisitions**

In the summer of 2002, simultaneous multiple-station observations of natural lightning discharges were conducted in the northeastern verge of Qinghai–Tibetan Plateau area in China (101°35′E, 37°33′N, 2650 m asl). Because of the special geography and topography of the area, thunderstorms, especially hailstorms, occurred there quite often. During the experiment, field mills, and fast and slow antenna systems were employed in 6 sites

synchronized by GPSs with a 0.4 μs time resolution. The time constants of the slow antenna and fast antenna systems were 6 s and 2 ms with a frequency bandwidth of 4 Hz ~ 2 MHz and 70 Hz ~ 5 MHz, respectively. Outputs of these antenna systems were digitized by a 16-bit A/D converter and recorded by a computer at a sampling rate of 4 MHz. The recorded length was 2 s per event. More detail description about the experiment was given by Qie et al. (2005). In following, 115 electric field change waveforms recorded by the slow antenna system at Liangjiao site for negative cloud-to-ground discharges on August 4 of 2002 are chosen for the analyses.

3.2 ***Recognition of return strokes***

As shown in Fig 1(a), the waveform of electric field changes produced by a return stroke usually has a distinct transition feature. Our study shows that this feature becomes much significant when the wavelet analysis is applied to the electric field waveform of the return stroke. By employing the Haar wavelet as the analysis wavelet, which is defined as

$$\psi(t) = \begin{cases} 1 & 0 \le t < 0.5, \\ -1 & 0.5 \le t < 1, \\ 0 & otherwise. \end{cases} \tag{7}$$

it is found the appropriate indicator for the return stroke electric field signal is the coefficient of variation C_V of wavelet coefficient, which is defined as $C_V = \sigma / \langle\tau\rangle$, where $\langle\tau\rangle$ and σ are the mean and standard deviation, respectively. The procedure of the wavelet analysis is as follows:

(i) Firstly, perform the wavelet multiresolution decomposition over the return stroke electric field signal as shown in Fig 1(a).

(ii) Secondly, analyze the evolution of the C_V and the mean $\langle\tau\rangle$ of the wavelet coefficient at the first level decomposition (D_1), using overlapping windows of 1024 points with a shift of 1 point. For each window the C_V and the mean $\langle\tau\rangle$ are calculated.

(iii) These calculated C_V and $\langle\tau\rangle$ values are then associated with the time of the last point in the window, and are plotted into diagrams as shown in Figs 1(b) and 1(c), respectively.

It is noted that the C_V waveform has a distinct step feature and a sharp peak (see Fig 1(b)) at the times as same as the fast transition and peak of the return stroke electric field waveform (see Figs 1(a)), while the mean value $\langle\tau\rangle$ increases steadily (see Fig 1(c)). This means that a return stoke may be recognized and distinguished more effectively and reliably by examining

the C_V and $<\tau>$ values of its electric field waveform. Similar results have been obtained for all other 114 cases, demonstrated the suitability of this method.

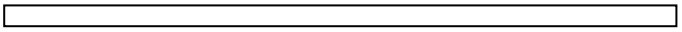

Fig. 1 Time variations of coefficients of the variation C_v (b) and the mean $<\tau>$ (c) of first level wavelet coefficients D_1 for the electric field signal of the first return stroke No. 163338 (a), dashed vertical line indicating the feature point of the return stroke.

3.3 ***Multifractal analysis***

Multifractal analysis has been performed for the electric field waveforms of the chosen 115 return strokes. The two-order Daubechies wavelet (Db2), which is characterized by four filter coefficients, was chosen to extract the fluctuations in the multifractal analysis. For convenience in comparison, all the partition functions $Z(q,s)$ were calculated for q varying between -5 and 7, and all the scaling exponents were determined by fitting in the regime $4 < s < N/2$, with $N = 2048$ as the length of the signal window of the return stroke on which the analysis was performed.

Fig. 2 shows the values of the exponents H_1 and H_2 for the same return stroke shown in Fig 1(a), which were estimated from the straight line fitting of $F_q(s)$ versus scale s for q = 1, 2, respectively. The Pearson correlation coefficients (r), which measure the goodness of the fitting, were as high as 0.99.

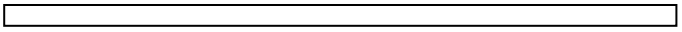

Fig. 2 Log-log plots of the fluctuation functions $F_1(s)$ and $F_2(s)$ versus scale s for the same return stroke shown in Fig.1(a). Solid lines represent the linear least square fitting curves, the calculated H_1 and H_2 were also reported in the figure.

The results of H_1 and H_2 for all other cases, which are very similar, are shown in Fig. 3. The error bars in the figure represent the standard deviation. It is noted that the exponents H_2 are all less than 0.5, thus no apparent long-range persistence exists in the whole process of a return stroke in term of the electric field waveform. The resultant power spectral exponent β, which is related to the H_2 by $\beta = 2H_2 + 1$, ranges from 1.6 to 2.0, with an average of 1.8. The fractal dimension D of the electric field signal of a return stroke can be estimated from H_1 by $D = 2 - H_1$. The D obtained ranges from 1.2 to 1.5 with an average of 1.3. On the other hand, the model work of Valdivia (1997) showed that the emission strength of lightning channel were sensitive to the fractal dimension of the discharge channel, which has an optimal

dimension of 1.3. Tsonis (1996] estimated that the average fractal dimension of cloud-to-ground lightning image is 1.34. Referring to the work of Vecchi et al. (1994) that the field radiated by a fractal channel appears to have same fractal dimension as the channel, our results here is consistent with them.

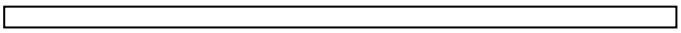

Fig. 3 The exponents H_1 and H_2 for the 115 return stroke signals analyzed, error bars representing the standard deviations.

The results of the multifractal spectrum $\tau(q)$ and corresponding singularity spectrum $f(\alpha)$, for the same signal shown in Fig. 1(a) are shown in Fig.4. It can be seen that the Renyi spectrum $\tau(q)$ is curved and the singularity spectrum $f(\alpha)$ is wide, indicating strong multifractal and nonlinear behavior of the return stroke. A modification of the binomial multiplicative cascade multifractal model by Kantelhardt et al. (2002) shows that the multifractal spectrum $\tau(q)$ of a signal with significant multifractal behavior fits to the formula

$$\tau(q) = -\frac{\ln(a^q + b^q)}{\ln 2} \qquad (8)$$

By least-square fitting of our $\tau(q)$ results to Eq. (8), the parameters a and b are obtained and are also reported in Fig. 4. It can be seen that in the whole q-range the Renyi exponents are fitted perfectly with the Eq. (8).

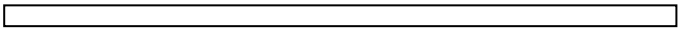

Fig. 4 Multifractal analysis of the return stroke electric field No. 163338: the Renyi exponents $\tau(q)$ and its fitting (solid line) with Eq.(8) (a), and the multifractal spectrum $f(\alpha)$ (b). The obtained two parameters a and b, and the corresponding α_{min} and $\Delta\alpha$ are reported in the figure also.

It can be easily derived that $\alpha(-\infty)=-(\ln a/\ln 2)$, corresponding to the weakest singularity α_{max}, and $\alpha(+\infty)=-(\ln b/\ln 2)$, corresponding to the strongest singularity α_{min}. The width of the singularity spectrum is $\Delta\alpha=\alpha_{max}-\alpha_{min}=\ln(b/a)/\ln 2$. As the $b\approx 1$, thus $\alpha_{min}\approx 0$, means that the singularity is close to that of the Heaviside step function. Meanwhile, the width $\Delta\alpha=1.5$ is very wide, indicating the high degree of multifractality of the return stroke signal analyzed.

The results of $\tau(q)$ and $f(\alpha)$ for all other cases are very similar. Fig.5 shows the histogram of α_{min} for all the 115 return strokes analyzed. A rather narrow range of the α_{min} around 0 can be observed, which implies a rather "stable" singularity feature of return stroke processes. We consider that the α_{min} may be a characteristic parameter relating the contact with ground in a return stroke process. The wide range of singular exponent $\Delta\alpha$ with the mean of 1.6, which implies the high degree of multifractality, may be another characteristic of the return stroke

process.

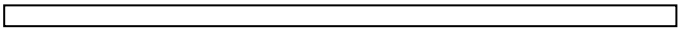

Fig. 5 The histogram of the α_{min} for the 115 return strokes analyzed.

3.4 ***Peak current and channel dimension of return strokes***

Let L represents the length of tortuous lightning channel of a return stroke and d the straight distance between two channel ends, there should be a relation $d \propto L^{1/D}$, referring to the perimeter maximum-diameter relation for measuring the fractal dimension by Mu et al. (1993), where D is the fractal dimension of the lightning channel. Bazelyan and Raizer (2000) show that the peak current of a return stroke is related to the cloud potential by $I_{rp} \propto U_c$, where U_c is cloud potential brought to the ground by leader.

Assuming that the leader tip potential, U_c, and the charge deposited in the leader channel, Q, are direct proportion to the straight length, d, and the tortuous length, L, of the lightning channel respectively, i. e. $U_c \propto d$ and $Q \propto L$, and relating to the relation $d \propto L^{1/D}$ above, we have

$$I_{rp} \propto Q^{1/D} = Q^{v} \qquad (9)$$

Similar formula to Eq. (9) were obtained by Berger (1972) and Cooray and Lundquist (1985). With the average $D=1.3$ obtained for 115 return strokes analyzed in above section, the v = 0.77, which is close to the values of Bergers'.

4. CONCLUSIONS

The fractal and scaling behaviors of the electric field waveforms produced by first return strokes were investigated with wavelet multiresolution based method. Totally 115 return strokes in negative cloud-to-ground discharges were studied. The major results include:

(a) Wavelet analyses show that the time evolution of the coefficient of variation of wavelet coefficients of the return stroke electric signal is characterized with a distinct step change and a sharp peak, which are similar to but more significant than those of the return stroke electric signal. This means that the coefficient of variation of the wavelet coefficients of the return stroke signal may be a more reliable indicator for recognition of return stokes.

(b) Multifractal analyses show that the return stroke electric signal exhibits strong degree

of multifractality and singularity. The fractal dimension of the signal ranges from 1.2 to 1.5 with an average of 1.3, which is very close to the fractal dimension of lightning channels obtained by others. The multifractal spectrum of the signal fits the modified version of binomial multifractal model very well. The multifractal spectrum may be regarded as the 'fingerprints' of return strokes, and in combination with the advantage of wavelet coefficients, it should be important in lightning automatic recognition and characterization.

(c) The peak current of a return stroke has been related to the charge deposited in the leader channel by using the fractal dimension obtained.

Lastly, the possible correction of scaling with log-periodic oscillator could be an important and interesting topic relating the branching processes underlying the structure of lightning.

ACKNOWLEDGMENTS

The work leading to this paper was supported by the National Natural Science Foundation of China (Grant No. 40605002, Grant No. 40575002) and the Research Committee of The Hong Kong Polytechnic University.

REFERENCES

Arneodo, A., Bacry, E., Muzy, J.F., 1995, The thermodynamics of fractals revisited with wavelets, Physica A, 213(1~2), 232-275.

Bazelyan, E.M., Raizer, Y.P., 2000, Lightning Physics and Lightning Protection, Institute of Physics Publishing: Philadelphia.

Bak P., Tang C., Wiesenfeld, K., 1987, Self-organized criticality: an explanation of 1/f noise. Phys. Rev. Lett. 59(4), 381~384.

Berger, K., 1972, Methoden und Resultate der Blitzforschung aufdem Monte San Salvatore bei lungano in den Jahren. 1963-1971, Bul. Swiss. Electrotech, 63, 1403-1422.

Cooray, V., Lundquist, S., 1985, Characteristics of the radiation fields from lightning in Sri Lanka in the Tropic, J. Geophys Res., 90 (D4), 6099-6109

Davis, A., Marshak, A., Wiscombe, W. et al., 1994, Multifractal Characterization of nonstationary and Intermittent geophysical fields: Observed, retrieved, or simulated. J. Geophys. Res., 99(D4), 8055-8072

Daubechies, I., 1992, Ten lectures on wavelets, SIAM, Philadelphia (1992), pp377.

Kantelhardt, J.W., S.A. Zschiegner, E.Koscielny-Bunde et al., 2002, Multifractal detrended fluctuation analysis of non-stationary time series, Physica A, 316, 87-114.

Kawasaki, Z., Matsuura, K., 2000, Does a lightning channel show a fractal? Applied Energy, 67(1-2), 147-158.

LeVine, D.M., Meneghini, R., 1978, Simulation of radiation from lightning return strokes: the effects of tortuosity, Radio Sci. 13 (5), 801–809.

LeVine, D.M., Willett, J. C., 1995, The influence of channel geometry on the fine structure of radiation field for lightning return strokes. J. Geophys. Res., 100 (D9), 18629-18638

Lupò, G., Petrarca, C. and Tucci, V., 2000, EM field associated with lightning channels: on the effects of tortuosity and branching, IEEE Trans. Electromagn. Compat., 42(4), 394-404.

Mallat S., A , 1999, Wavelet Tour of Signal Processing, 2nd Edition, Academic Press, San Diego (1999), pp620.

Manimaran, P., Panigrahi, P.K., and Parikh, J.C., 2005, Wavelet Analysis and scaling properties of time series, Phys. Rev. E 72, 046120/1-5.

Manimaran, P., Panigrahi, P.K., and Parikh, J.C., 2006, Multiresolution analysis of fluctuations in non-stationary time series, *eprint: nlin.CD/0601065*

Peng, C.K., Buldyrev, S.V., Havlin, S., et al., 1994, Mosaic organization of DNA nucleotides, Phys. Rev. E 49, 1685 - 1689

Qie, X., Kong, X., Zhang, G. et al., 2005, The possible charge structure of thunderstorm and lightning discharges in northeastern verge of Qinghai–Tibetan Plateau, Atmospheric Research, 76, 231–246.

Sornette, D., 2002, Predictability of catastrophic events: Material ruptures, earthquakes, turbulence, financial crashes, and human birth, PNAS, USA, 99, 2522-2529.

Sornette, D., 2004, Critical Phenomena in Natural Sciences (Chaos, Fractals, Self-organization and Disorder: Concepts and Tools), 2nd ed., Springer Series in Synergetics (Springer-Verlag, Heidelberg) (2004).

Tan Y., Tao, S. Zhu, B. 2006, Fine resolution simulation of the channel structures and propagation features of intracloud lightning, Geophys. Res. Lett., 33(9), L09809 DOI: 10.1029/2005GL025523

Tsonis, A.A., 1996, A fractal study of dielectric breakdown in the atmosphere, Proceedings of 10th International Conf on Atmospheric Electricity, ICAE, Osaka, Japan, 345-348.

Turcotte, D.L., Malamud, B.D., Guzzetti, F., and Reichenbach, P., 2002, Self-organization, the cascade model, and natural hazards, PNAS 99, 2530-2537.

Weidman, C.D., Krider, E.P., 1978, The fine structure of lightning return stroke wave forms, J Geophys Res., 83, 6239~6247.

Vecchi, G., Labate, D. Canavero, F., 1994, Fractal approach to lightning radiation on a tortuous channel, Radio Sci. 29(4), 694-704.

Valdivia, J.A, Milikh, G.M, Papadopoulos, K., 1997, Red sprites: Lightning as a fractal antenna, Geophys. Res. Lett., 24(24), 3169-3172.

Uman, M.A., 2001, The Lightning Discharge, Dover Publications，Mineola New York (2001), pp377.

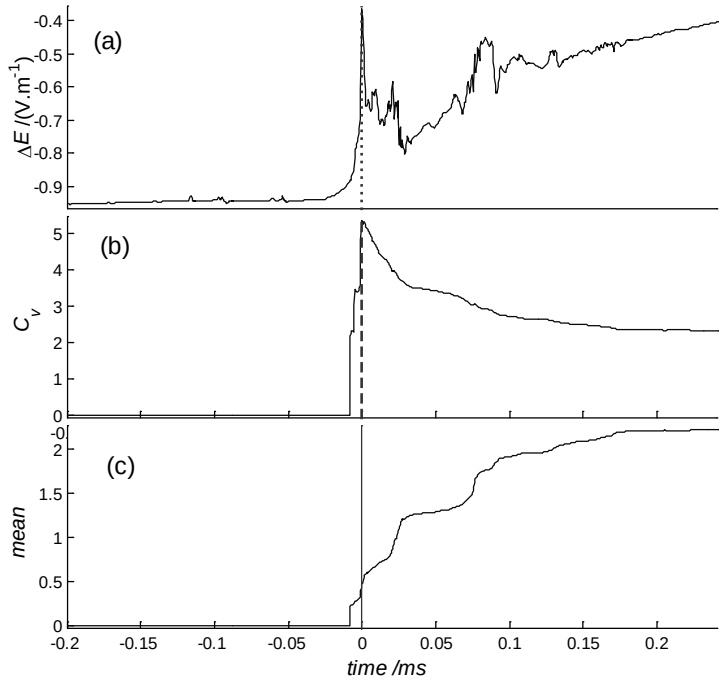

Fig. 1 Time variations of coefficient of the variation C_v (b) and the mean $<\tau>$ (c) of first level wavelet coefficients D_1 for the electric field signal of the first return stroke No. 163338 (a), dashed vertical line indicating the feature point of the return stroke.

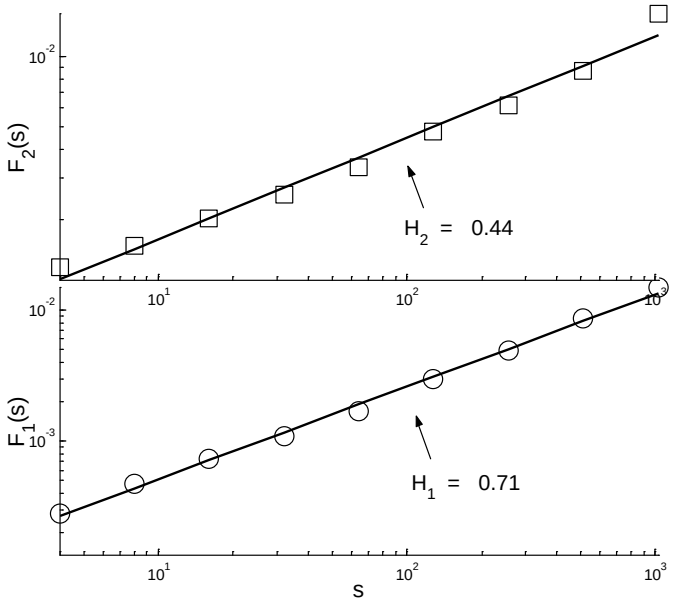

Fig. 2 Log-log plots of the fluctuation functions $F_1(s)$ and $F_2(s)$ versus scale s for the same return stroke in Fig.1(a). Solid lines represent the linear least square fitting, the obtained H_1 and H_2 were reported in the figure.

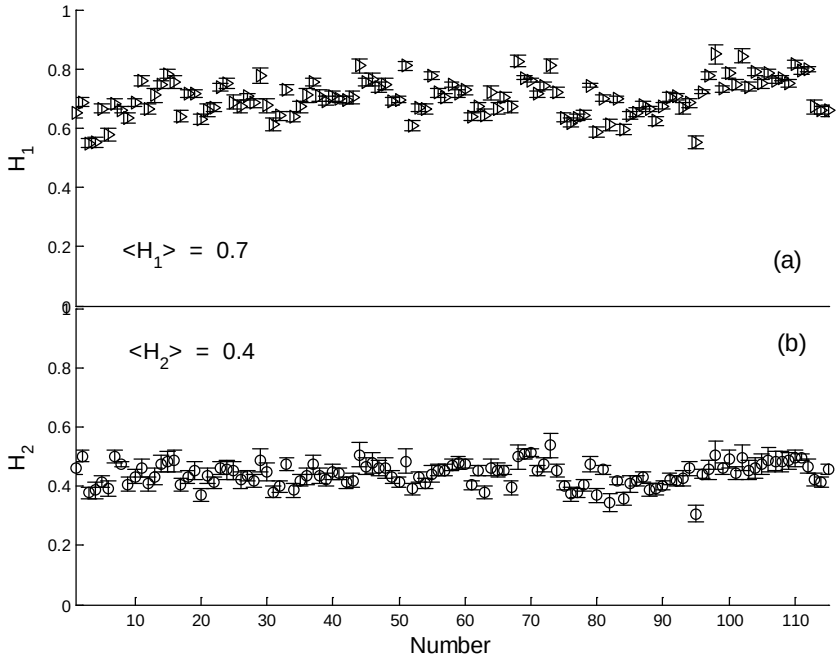

Fig. 3 The exponents H_1 and H_2 for the 115 return strokes analyzed, error bars representing the standard deviations.

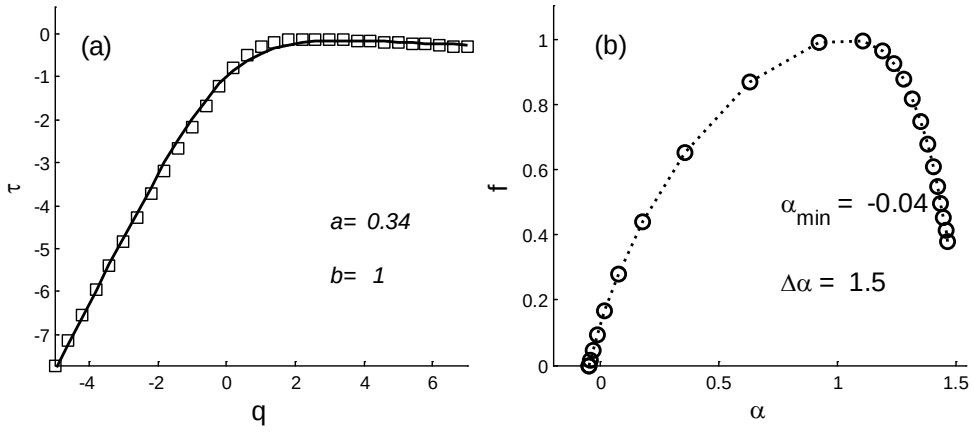

Fig. 4 Multifractal analysis of the return stroke electric field No. 163338: the Renyi exponents $\tau(q)$ and its fitting (solid line) with Eq.(8) (a), and the multifractal spectrum $f(\alpha)$ (b), The obtained two parameters a and b, and the corresponding α_{min} and $\Delta\alpha$ are reported in the figure also.

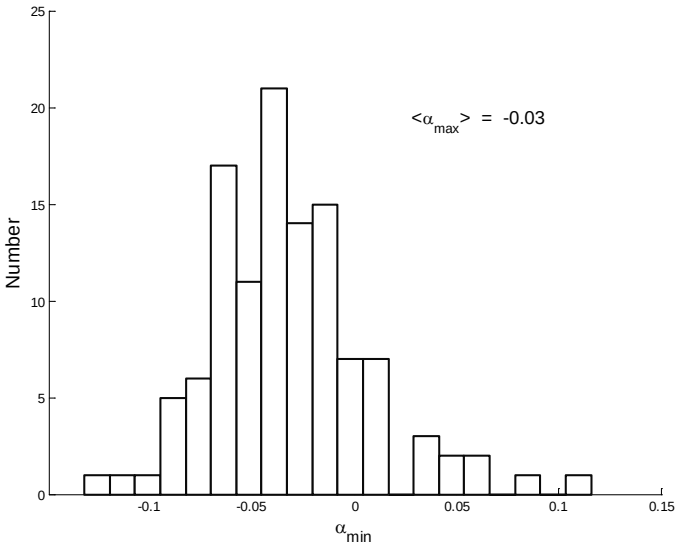

Fig. 5 The histogram of the minimum exponent α_{min} for the 115 return strokes analyzed.

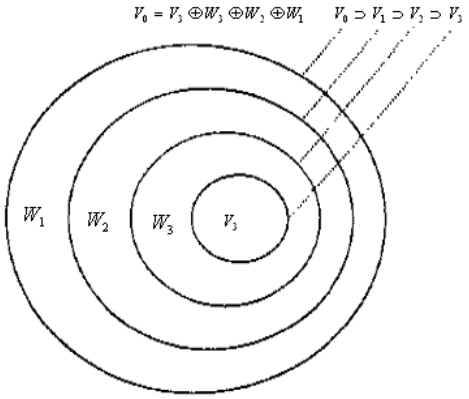

Fig. 6 Illustration of wavelet spaces and the containment of scale spaces

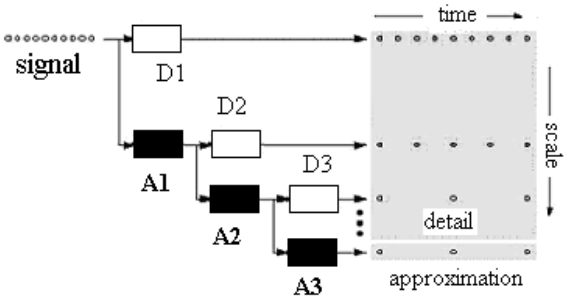

Fig. 7 A diagram of the wavelet multiresolution decomposition of a signal

APPENDIX

Wavelet theory with its roots in the classical Fourier analysis can be thought as a refinement of the Fourier analysis and has been widely applied in a variety of engineering and science disciplines. Basis functions of the wavelets are produced from two mutually orthogonal companion functions, the father wavelet (or scaling function) $\phi(t)$ and the mother wavelet (or wavelet function) $\psi(t)$, by the operation of scaling (dilation) and translation (shift), here $\phi(t)$ and $\psi(t)$ are square integral real functions ($\in L^2(R)$) satisfying $\int \phi(t)dt = 1$ and $\int \psi(t)dt = 0$ (Daubechies, 1992; Mallat, 1999).

The heart of wavelet analysis is multiresolution analysis (MRA), which is essentially characterized by scaling function. A multiresolution analysis of $L^2(R)$ associated with the scaling function $\phi(t)$ is defined as a nested chain of closed subspaces: $\ldots \subset V_2 \subset V_1 \subset V_0 \subset V_{-1} \subset \ldots$ such that $V_\infty = \{0\}$ and $V_{-\infty} = L^2(R)$, and the additional condition $f(t) \in V_j \Leftrightarrow f(\frac{t}{2}) \in V_{j+1}$ $j \in Z$, here V_j is the subspace spanned by $\{\varphi_{j,k}(t) = 2^{-\frac{j}{2}}\varphi(2^{-j}t - k) \quad k \in Z\}$, Z presents the set of integers.

The association of mother wavelet $\psi(t)$ with multiresolution analysis is such that the sets $\{\psi_{j,k}(t) = 2^{-\frac{j}{2}}\psi(2^{-j}t - k) \quad k \in Z\}$ form an orthonormal basis of the orthogonal supplement W_j of V_j in V_{j-1} that is, $V_{j-1} = V_j \oplus W_j$ $j \in Z$, thus the V_0 space can be decomposed in the way $V_0 = (\overset{J}{\underset{j=1}{\oplus}} W_j) \oplus V_J$ by simply iterating the decomposition j times, here J is an arbitrary lowest resolution level. The subspace sequences $\{V_j, \ j \in Z\}$ and $\{W_j \quad j \in Z\}$ of $L^2(R)$ are called approximation and detail spaces, respectively. The wavelet spaces and the containment of scale spaces are shown in Fig. 6

The approximation of a signal $f(t)$ at the resolution 2^j is given by its orthogonal projection onto the subspace V_j, $A_j = \sum_{k=-\infty}^{\infty} < f, \phi_{j,k} > \phi_{j,k}$, here $<\cdot,\cdot>$ denotes an inner product, and the smaller the j, the finer the resolution obtained. The additional details needed for

increasing the resolution for $2^{-\frac{j}{2}}$ to $2^{-\frac{j+1}{2}}$ are given by the orthogonal projection D_j of the signal onto W_j: $D_j = \sum_{k=-\infty}^{\infty} < f, \psi_{j,k} > \psi_{j,k}$, and the relationship between the successive approximation A_j and A_{j+1} is summarized by $A_j = A_{j+1} + D_{j+1}$, there exists a cascaded decomposition technique, termed multiresolution signal decomposition. At each resolution level j, the approximation A_j can be decomposed into smooth part A_{j+1} and detail part D_{j+1}. Let 0 and J be the highest and lowest resolution level of the signal $f(t)$, then $f(t)$ can be decomposed into coarse approximation (smooth background) and a series of detail signals (fluctuation) $f(t) = A_J + \sum_{1}^{J} D_j$ (see illustration of Fig. 7).

Since both the scaling function $\phi(t)$ and the mother wavelet $\psi(t)$ belong to V_{-1}, and $\{\phi_{-1,k}(t) = \sqrt{2}\phi(2t-k)\}$ is an orthonormal basis for V_{-1}, one obtains a two level relation $\phi(t) = \sqrt{2}\sum_k h_k \phi(2t-k)$ and $\psi(t) = \sqrt{2}\sum_k g_k \phi(2t-k)$, here h_k and g_k are pair of low-pass and high-pass quadrate mirror filters such that $g_k = (-)^k h_{1-k}$. The wavelet multiresolution decomposition process can be viewed as application of the pair of filters first to the original signal, and then recursively to the approximation series only. At each level of decomposition *j*, the high-pass filter is associated with the wavelet function $\psi_{j,k}(t)$, whereas the low-pass filter is associated with the scaling function $\varphi_{j,k}(t)$. Hence, wavelet functions describe high-frequency signal components, while scaling functions describe smooth components.

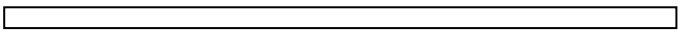

Fig. 6 Illustration of wavelet spaces and the containment of scale spaces

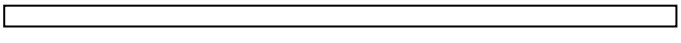

Fig. 7 A diagram of the wavelet multiresolution decomposition of a signal